Nanoscale

PAPER

View Article Online
View Journal | View Issue

Cite this: *Nanoscale*, 2024, **16**, 6268

Selenium reduction pathways in the colloidal synthesis of CdSe nanoplatelets†

Alessio Di Giacomo,[a] Alina Myslovska,[a] Vic De Roo, [b] Jan Goeman,[b] José C. Martins [b] and Iwan Moreels [*a]

Several established procedures are now available to prepare zinc blende CdSe nanoplatelets. While these protocols allow for detailed control over both thickness and lateral dimensions, the chemistry behind their formation is yet to be unraveled. In this work, we discuss the influence of the solvent on the synthesis of nanoplatelets. We confirmed that the presence of double bonds, as is the case for 1-octadecene, plays a key role in the evolution of nanoplatelets, through the isomerization of the alkene, as confirmed by nuclear magnetic resonance spectroscopy and mass spectrometry. Consequently, 1-octadecene can be replaced as a solvent (or solvent mixture), however, only by one that also contains α protons to C=C double bonds. We confirm this *via* synthesis of nanoplatelets in hexadecane spiked with a small amount of 1-octadecene, and in the aromatic solvent 1,2,3,4-tetrahydronaphthalene (tetralin). At the same time, the chemical reaction leading to the formation of nanoplatelets occurs to some extent in saturated solvents. A closer examination revealed that an alternative formation pathway is possible, through interaction of carboxylic acids, such as octanoic acid, with selenium. Next to shedding more light on the synthesis of CdSe nanoplatelets, fundamental understanding of the precursor chemistry paves the way to use optimized solvent admixtures as an additional handle to control the nanoplatelet synthesis, as well as to reduce potential self-polymerization hurdles observed with 1-octadecene.

Received 12th October 2023,
Accepted 21st February 2024

DOI: 10.1039/d3nr05157a

rsc.li/nanoscale

Introduction

Starting with the pioneering work of Murray *et al.* in 1993,[1] colloidal semiconductors with nanometer dimensions gained progressively more attention, nowadays reaching marketable technological applications such as displays, photodetectors or energy harvesters.[2,3] The progress in synthetic procedures over the last three decades has allowed continuous improvement of control over size, size dispersion, and shape, yielding tailored optoelectronic properties and, at the same time, a detailed understanding of the associated nucleation and growth mechanisms.

A first, and key step in the synthesis process is given by the formation of monomers from suitable metal and pnictogen,[4] chalcogen,[5,6] or halogen[7] precursors. The monomer formation rate determines the monomer supersaturation in solution, and consequently the critical size of nuclei as well as the final nanocrystal size, size dispersion and concentration.[8] Focusing, in the context of this work, on metal chalcogenide nanocrystals, initial studies targeted the mechanistic understanding of the nanocrystal synthesis using phosphine chalcogenides,[5,9] yet, in an effort to avoid phosphine-based solvents and precursors, attention rapidly shifted to 1-octadecene (ODE).

The earlier literature often referred to it as a noncoordinating solvent.[10–12] On the other hand, the reactivity of chalcogens with carbon–carbon double bonds is well known and also industrially exploited, with vulcanization processes (production of hard crosslinked rubbers) being the best example.[13] Also for the CdSe quantum dot synthesis, it was rapidly realized that ODE can yield a source of reactive selenium.[14–16] Upon further investigation of the nature of the chalcogen precursor in ODE, Deng *et al.*[17] demonstrated that dehydrogenation of saturated alkane molecules at elevated temperature, of 300 °C, can lead to the formation of H_2Se. Others, studying either formation of H_2S[15] or H_2Se[16] confirmed that this mechanism is also present in ODE, albeit with a reduced yield compared to a saturated alkane.[17] These results align well with the notion that selenium can be used as a dehydrogenating agent in the determination of natural products' structures, as well as in the aromatization step of complex molecules.[18,19] In addition to the formation of H_2Se, Bullen *et al.*[20] observed that

[a]*Department of Chemistry, Ghent University, 9000-Gent, Belgium. E-mail: iwan.moreels@ugent.be*
[b]*Department of Organic and Macromolecular Chemistry, Ghent University, 9000-Gent, Belgium*

†Electronic supplementary information (ESI) available: Additional TEM images, ^{1}H, ^{1}H–^{1}H COSY and ^{1}H–^{13}C HSQC NMR spectra of precursors and solvents, mass spectra of precursors, photographs of precursor solutions. See DOI: https://doi.org/10.1039/d3nr05157a

a different source of reactive Se is produced through isomerization of the double bond in ODE, leading to reactive ODE_x-Se_y species. In conclusion, the key observation is that all these reactions reduce metallic Se^0 to Se^{2-}, a prerequisite to obtain the CdSe monomers.

Among the various nanocrystal shapes that can be produced at present, nanoplatelets (NPLs) have recently emerged as an exciting class of materials. The quantum confinement along their thickness direction is defined by the number of N monolayers (MLs, where the N Se crystalline planes are bound to $N + 1$ planes of Cd), and is tunable with atomic precision.[21] The resulting NPLs possess peculiar optoelectronical properties compared to 0D quantum dots, such as a faster photoluminescence (PL) decay,[22] narrower emission line widths, and higher optical gain coefficients,[23,24] making them potential candidates for efficient light-emitting diodes or lasers.[24–28]

Established procedures to synthesize NPLs are mostly based on metal carboxylates as precursors and Se dissolved in ODE, and yield highly luminescent zinc blende CdSe NPLs with precise control over their thickness and lateral dimensions.[29–35] The approach can be generalized by the following chemical reaction:

$$\mathrm{Cd(OOCR)_2 + Se + ODE} \xrightarrow[\text{short-chained ligand}]{\Delta T} \mathrm{CdSe\ NPLs} \quad (1)$$

ΔT refers to the high temperatures, typically exceeding 200 °C, required in these syntheses. In addition, short-chained cadmium carboxylates[36] or carboxylic acids[34] are added after nucleation of small CdSe seeds to promote lateral growth of 2D nanocrystals. Several synthetic protocols allow for control over the structural and optoelectronic properties of the resulting NPLs,[21] but the underlying chemistry remains somewhat ill-defined. In eqn (1), one can notice that the metallic Se^0 is employed, which should again be reduced to Se^{2-}. As the metal center retains its oxidation state, the likely redox partner is again ODE.

Considering its central role in the CdSe NPL synthesis, and that recently, practical concerns about the usage of ODE were reported, in particular its ability to form polymers of sizes comparable to the nanocrystals, which can hamper proper sample purification,[37,38] we have investigated the precursor chemistry behind the synthesis of CdSe NPLs. Focusing on the behavior of ODE in the presence of Se, we confirm the active participation of the C=C double bond in our synthesis, however, here not leading to H_2Se, but yielding $(ODE–Se)_2$. We also demonstrate that an alternative pathway exists *via* a reaction with carboxylic acids, leading to Se_x anhydride complexes, further enriching the reaction pathways. We finally demonstrate that we can perform the synthesis in alternative solvents, such as saturated alkanes (hexadecane) spiked with small amounts of ODE, or in aromatic solvents (tetralin), both providing a source of C=C double bonds without requiring ODE as main solvent.

Experimental

Materials

Cadmium oxide (≥99.99%), sodium myristate (Na(myr), ≥99%), octanoic acid (≥98.0%), 1,2,3,4-tetrahydronaphthalene (tetralin, synthesis grade) and chloroform-d ($CDCl_3$, d, 99.8%) were purchased from Merck/Sigma-Aldrich. *n*-Hexadecane (HD, 95%) was purchased from Fiers. 1-Octadecene (ODE, 90%), oleic acid (OA, 90%) were purchased by Alfa Aesar. Cadmium nitrate tetrahydrate (99+%), propionic acid (99.5+%), toluene (>99%), methanol (99.8+%) and 2-propanol (IPA, 99+%) were purchased from Chem Lab. Acetonitrile (ACN, 99.9%) was purchased from Carl-Roth. Selenium powder (≥99.99%) and cadmium acetate dihydrate 98% were purchased by Acros Organics. All chemicals were used without further purification. A vacuum/dry nitrogen gas Schlenk line was used for nanocrystal syntheses. The purifications were conducted in air unless specified otherwise.

Cadmium octanoate preparation ($Cd(oct)_2$)

The cadmium precursor was prepared according to a reported procedure.[34] Briefly, in a three-neck flask, 2.0 g (15.7 mmol) of CdO was added to 6.5 mL (41 mmol) of octanoic acid. While stirring, the system was heated under N_2 atmosphere to 180 °C, until a colorless solution is obtained. The reaction was kept at 180 °C for 20 minutes and then cooled. During cooling, between 110 °C and 80 °C, the mixture was connected to a vacuum line to remove the water produced in the condensation reaction. The colorless solution was rapidly transferred to centrifugation tubes, acetone was added and a white solid was precipitated after centrifugation. The solid fraction was centrifuged with fresh acetone three additional times to purify the reaction product, then dried overnight under vacuum.

Cadmium myristate preparation ($Cd(myr)_2$)

6 g of cadmium nitrate tetrahydrate were mixed with 400 mL of methanol using a stirring bar. Separately, 10 g of $Na(myr)_2$ were mixed with 300 mL of methanol and sonicated for an hour. The Cd solution was then added dropwise to the myristate precursor over a period of approximately 4 hours, while stirring. The mixture was then filtered using a Buchner funnel in a Buchner flask connected to the Schlenk line. The final product was dried overnight under vacuum.

Cadmium oleate preparation ($Cd(OA)_2$ in ODE)

In a three-neck round bottom flask CdO (15 mmol) was added to OA (45 mmol) and ODE (15 mL). The mixture was degassed under vacuum at 80 °C for 1 hour. Under nitrogen, the mixture was heated to 200 °C for 15 minutes, until full dissolution of the solid. After removing the thermomantle the mixture was allowed to cool down and finally transferred into vials for storage.

Synthesis of ODE–Se reagent

The selenium precursor was prepared according to a reported procedure.[20] In a 25 mL three-neck flask 1.02 mmol of sel-

enium powder and 10 mL of ODE were added. The system was placed under N_2 and then heated to 200 °C for 2 h. A yellow solution was formed. The reaction mixture was transferred in glovebox and passed through a 450 μm pore size syringe filter to remove eventual unreacted selenium mesh. The reagent was stored in glovebox.

Synthesis of OctAc–Se reagent

In a 25 mL round bottom flask, 1.25 mmol of selenium was added to 10 mL of octanoic acid. The suspension was degassed for 1 h at 100 °C, followed by heating, under N_2, to 160 °C for 60 minutes. The temperature was then set to 220 °C for 30 minutes, followed by 230 °C for 30 minutes, until everything dissolved. An orange solution was obtained, which upon cooling down turned grey. The reaction mixture was transferred to a glovebox and passed through a 450 μm pore size syringe filter to remove unreacted selenium mesh. A pale yellow solution was obtained.

Synthesis of 3.5 ML CdSe NPLs with $Cd(oct)_2$ in different solvents

The NPLs were prepared with slight modifications to a procedure reported elsewhere.[34] Briefly, in a 25 mL three-neck flask 0.50 mmol of $Cd(oct)_2$ and 0.26 mmol of Se powder were mixed with *ca.* 12 mL of the solvent of choice. Four different trials were conducted: HD (12 mL, 40.8 mmol), ODE (12 mL, 37.5 mmol), HD + ODE (two different runs: 40.8 mmol HD + 0.06 mmol ODE and 40.8 mol HD + 0.5 mmol ODE, respectively) and tetralin (12 mL, 88.0 mmol). The suspension was degassed for 1 h at 100 °C, followed by heating the mixture, under N_2, to 160 °C for 10 minutes. The temperature was then set to 220 °C and, at 200 °C, 100 μL (1.33 mmol) of propionic acid dispersed in 1 mL of HD, was swiftly injected. The reaction proceeded for 20–185 minutes at 220 °C, then heating was removed to cool the system. When the temperature reached 160 °C, 0.80 g of $Cd(OA)_2$ in ODE was injected, the suspension was cooled to 80 °C and the mixture transferred into vials to proceed with purification.

Synthesis of CdSe NPLs with $Cd(oct)_2$ and ODE–Se reagent

The synthesis of CdSe was conducted following the same procedure described previously in HD (12 mL, 40.8 mmol), but replacing selenium mesh with the equimolar amount of ODE–Se solution (2.5 mL, 0.25 mmol Se). The purification was conducted according to the protocol described below.

Synthesis of CdSe NPLs with $Cd(oct)_2$ and OctAc–Se reagent

The synthesis followed the same procedure as for ODE–Se, but with 199.4 mg $Cd(oct)_2$, 2.6 mL of OctAc–Se and 9.4 mL of HD. The growth time was set at 60 minutes.

General purification protocol for CdSe NPLs

The crude synthesis product was mixed with 15 mL toluene and 10 mL of a 1.5 : 1 (v/v) solution of IPA : ACN was added. The suspension was centrifuged for 10 minutes at 4500 rpm. The supernatant was discarded, the solid was redispersed in toluene and the precipitation was repeated twice. The final solid was dispersed in 5 mL hexane and centrifuged at 4200 rpm to remove unreacted carboxylates. The solid was discarded and the supernatant, containing CdSe NPLs, was collected and stored in hexane.

Specific purification of CdSe NPLs synthesized in tetralin

We applied the general procedure above, however, in the last step, we collected the precipitate containing CdSe NPLs, and stored it in hexane.

Synthesis and purification of 2.5 ML CdSe NPLs

In a 25 mL three-neck flask, 0.50 mmol of $Cd(oct)_2$ and 0.26 mmol of Se powder were mixed with 12 mL of HD. The suspension was degassed for 1.5 h at 100 °C, followed by heating the mixture, under N_2, to 160 °C for 10 minutes. The temperature was then set to 190 °C and, at 170 °C, 100 μL of propionic acid dispersed in 1 mL of HD, was swiftly injected. After 30 minutes, heating was removed to cool the system, and 1 mL of a 0.5 M $Cd(OA)_2$ solution in ODE was injected, the suspension was cooled to 80 °C and the mixture transferred into vials to proceed with purification.

The crude synthesis product was first centrifuged at 2500 rpm for 10 minutes. The supernatant was retained, 1.2 mL of IPA and 6 mL of EtOH were added, the mixture was centrifuged for 5 minutes at 5000 rpm and the resulting precipitate was redispersed in hexane.

Synthesis and purification of 5.5 ML CdSe NPLs

In a 25 mL three-neck flask, 0.30 mmol of $Cd(myr)_2$ was dissolved in 12 mL of hexadecane. The solution was degassed for 1.5 h at 100 °C, followed by heating, under N_2, to 250 °C. At that temperature, 24.5 mg of Se-mesh (0.31 mmol) in a mixture of 800 μL of HD and 192 μL of ODE (0.6 mmol) were injected. After one minute, 144 mg of $Cd(Ac)_2{\cdot}2H_2O$ was inserted. The reaction proceeded for an additional 440 seconds, then the heating was removed, 300 μL of 0.5 M Cd $(OA)_2$ in ODE was injected, and the reaction mixture was cooled with in a water bath.

To purify the NPLs, 10 mL of the crude synthesis product was mixed with 20 mL hexane, 200 μL of oleic acid, 10 mL of IPA and 5 mL of EtOH. The suspension was centrifuged at 4800 rpm for 5 minutes. The precipitate was redispersed in 10 mL of hexane and centrifuged at 3000 rpm for 10 minutes. Finally, the precipitate was discarded, and the supernatant was stored.

Heating up of HD, ODE, and octanoic acid with selenium

In a 25 mL round bottom flask 1.25 mmol of Se was added to 10 mL of the solvent. The suspension was degassed for 1 h at 100 °C, followed by heating the mixture, under N_2, to 160 °C for 10 minutes. The temperature was then set to 220 °C for 30 minutes. While hexadecane remained colorless, deep orange suspensions were obtained for ODE and octanoic acid. The solvents turned orange (ODE) and pale yellow (octanoic acid) after returning to room temperature. The reaction mix-

tures were transferred in a glovebox and passed through a 450 μm pore size syringe filter to remove eventual unreacted selenium mesh. The final products were stored in a glovebox.

Transmission electron microscopy

Samples were prepared by drop-casting dilute *n*-hexane dispersions onto carbon-coated copper grids. Bright field TEM images were acquired on a JEOL JEM-1011 microscope (W filament) operating at an accelerating voltage of 100 kV.

Optical characterization

Absorbance spectra were taken with a PerkinElmer Lambda 950 spectrometer. Photoluminescence measurements were performed on an Edinburgh Instruments FLSP920 UV–Vis–NIR spectrofluorometer, using a 450 W xenon lamp as the excitation source.

NMR characterization

NMR measurements were recorded on a Bruker Avance III spectrometer operating at a ^{1}H frequency of 500.13 MHz and equipped with a BBI-Z probe. Samples for nuclear magnetic resonance were dispersed in $CDCl_3$. The sample temperature was set to 298 K. Standard pulse sequences as present in the Bruker library were used throughout. ^{1}H and ^{13}C chemical shift scales were calibrated by using the residual solvent signal as a secondary reference against TMS.

Liquid and gas chromatography, coupled with mass spectrometry

LC-MS analysis was performed on an Agilent (Santa Clara, CA, U.S.A) 1100 Series HPLC coupled to an Agilent G1946C MS detector equipped with an electrospray ionization source, using a Kinetex column (C18, 150 × 4.60 mm, 5 μm particle size). The flow rate was 1.5 mL min^{-1} using a gradient consisting of 5 mM NH_4OAc in H_2O and CH_3CN. Optimized gradients were used for each CLiP. GC-MS analysis was performed on an Agilent G1800B GC-MS system equipped with an electron ionization source, using a SSL inlet and helium as carrier gas.

Results and discussion

Our study conveys a description of the ODE reactivity in the synthesis of CdSe NPLs. In this study we have worked under reaction conditions used for the synthesis of 3.5 monolayer (ML) thick CdSe NPLs, recently reported.[34] We refer to our earlier work for the characterization of the reference NPLs,[34] and summarize the procedure in eqn (2):

$$\mathrm{Cd(OOCR)_2 + Se + solvent} \xrightarrow[(2)]{(1)} \mathrm{3.5\,ML\,CdSe\,NPLs} \quad (2)$$
$$(1) = 200\,^{\circ}\mathrm{C},\ \mathrm{CH_3CH_2COOH},\ (2) = 220\,^{\circ}\mathrm{C},\ 20\ \mathrm{min}$$

Step (1) consists of raising the precursor mixture to a temperature of 200 °C, inducing a nucleation of CdSe seeds, and subsequently adding propionic acid to promote lateral growth. The NPLs are further grown in step (2), at 220 °C for 20 minutes. Cadmium octanoate ($Cd(oct)_2$) was used as a metal precursor, as the chemical yield in NPLs is expected to be higher compared to other carboxylates.[34] The investigation aimed to pinpoint the role of the C=C double bond moiety in the reaction. If the alkene behaves simply as a noncoordinating solvent, one can rationalize that a solvent with comparable polarity and viscosity would not heavily impact the synthesis. Additionally, the potential self-polymerization issue in ODE[37] could be completely avoided using a fully saturated alkane. We selected *n*-hexadecane (HD) as an alternative to ODE, as this solvent was recently demonstrated to be a viable medium for different nanocrystal syntheses.[37,39]

Working in identical conditions as in eqn (2), but changing the solvent composition to HD, Fig. 1 demonstrates that the synthesis progression in the two media is noticeably different. In particular, while in ODE the expected 3.5 ML NPLs with a band gap around 460 nm are readily formed after 120 seconds[40] (Fig. 1a), in HD mainly 2.5 ML NPLs with a band gap around 390 nm (ref. 40) are formed (Fig. 1b), in addition to a small fraction of 3.5 ML NPLs and a broad background presumably due to scattering from large sheets.[34,41,42] We infer that the different reactivity of the selenium precursor in the presence of ODE can be the explanation for the observed behavior. To strengthen this hypothesis, we have registered control experiments in which we have added known amounts of ODE (0.06 mmol and 0.5 mmol, respectively) to the HD solvent (12 mL, 40.8 mmol). The results are reported in Fig. 1c and d. Even with the small ODE amounts used, the spectra show a reduced background absorption and a relative intensity increase of the signals related to 3.5 ML NPLs, compared to 2.5 ML NPLs. This already suggests that the presence of the carbon–carbon double bond moiety causes ODE to partake in the NPL reaction, and that higher ODE concentrations increase the overall reaction rate, including the transformation rate from 2.5 ML to 3.5 ML NPLs *via* Ostwald ripening.[43] ODE being a reagent has a double importance: firstly, it adds another layer of complexity to the system, as its concentration influences the evolution of the reaction. This information can be used for the optimization of the synthesis conditions *e.g.*, to stabilize different NPL populations at given reaction temperatures. On the other hand, reducing the amount of ODE could reduce the potential self-polymerization issue that was discussed earlier by Dhaene *et al.*[37]

As for the reactivity, it was suggested that the naturally occurring polynuclear selenium can form complexes of nucleararity Se_x (x = 2–3) when treated at high temperatures ($T \geq$ 200 °C) with species containing alkene protons, and radical mechanisms were suggested to take place in these conditions.[18,19,44,45] To address the solvent-chalcogen reactivity, we heated mixtures of selenium and ODE or HD under the same conditions as in eqn (2), and we sampled the reaction mixture *via* nuclear magnetic resonance (NMR) spectroscopy. The ^{1}H spectrum of the heated HD-Se mixture proved to be identical to the pristine HD (ESI, Fig. S1†), indicating that HD remains unaltered during heating. In agreement with this, no noticeable color change was observed after the heating (ESI,

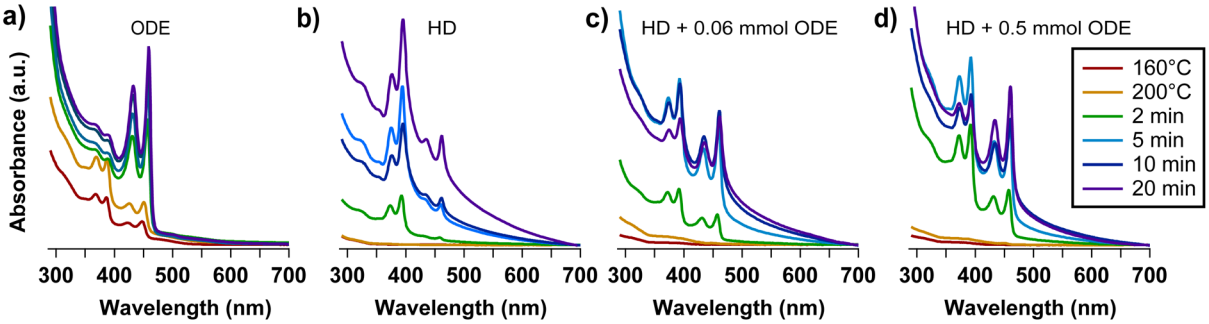

Fig. 1 Temporal evolution the absorption spectrum of aliquots collected during NPL synthesis performed under conditions as in eqn (2), using different solvents. (a) ODE (12 mL, 37.5 mmol, reproduced from ref. 34), (b) *n*-hexadecane (HD, 12 mL, 40.8 mmol), and (c) and (d) HD with known amounts of ODE added (HD + 0.06 mmol ODE and HD + 0.5 mmol ODE, respectively).

Fig. S2†). It has been reported in CdX (X = S, Se) syntheses that, starting from elemental chalcogens in saturated hydrocarbon solvents, reactive H_2X evolved accompanied by the dehydrogenation of the alkane to alkene.[15,17,46] The absence of signals in the characteristic alkene chemical shift region of 5.0–6.0 ppm discards this possibility under the synthesis conditions used in our work. Additionally, a test with $Pb(OAc)_2$ doped paper did not show any precipitate (PbSe). Hence, we did not observe any evidence of selenium reduction from the HD solvent in our experiments.

On the other hand, ODE displays a different behavior. After mixing selenium with ODE, the mixture evolves from colorless to dark orange at high temperatures, turning dark yellow after returning to room temperature (ESI, Fig. S2†). Fig. 2 shows the ^{1}H and ^{13}C NMR spectra of the heated mixture of Se and ODE. In the ^{1}H spectra, new resonances are now visible. First, the emerging multiplet appearing around 5.4 ppm (α in Fig. 2b) can be attributed to the presence of non-terminal alkene protons.[20] This is due to the formation of additional double bonds, *e.g.*, octadec-1,3-diene, or to the formation of C=C isomers, *e.g.*, 2-ODE, 3-ODE and related organoselenium complexes. Both options are reported in literature when double bonds with available allylic protons react with selenium at high temperature.[18,20,44] The new signals appearing in the region 1.55 ppm–1.75 ppm (ε, ϕ, γ of Fig. 2c) are compatible with allylic CH_3 or CH_2 in β position to a double bond. Furthermore, the additional resonance appearing around 1.95 ppm (η in Fig. 2c) is compatible with the presence of a CH_2 in allylic position to the isomerized double bond, *e.g.*, $CH_3CH{=}CH\text{-}CH_2R$ in 2-ODE, as well as to a related organose-

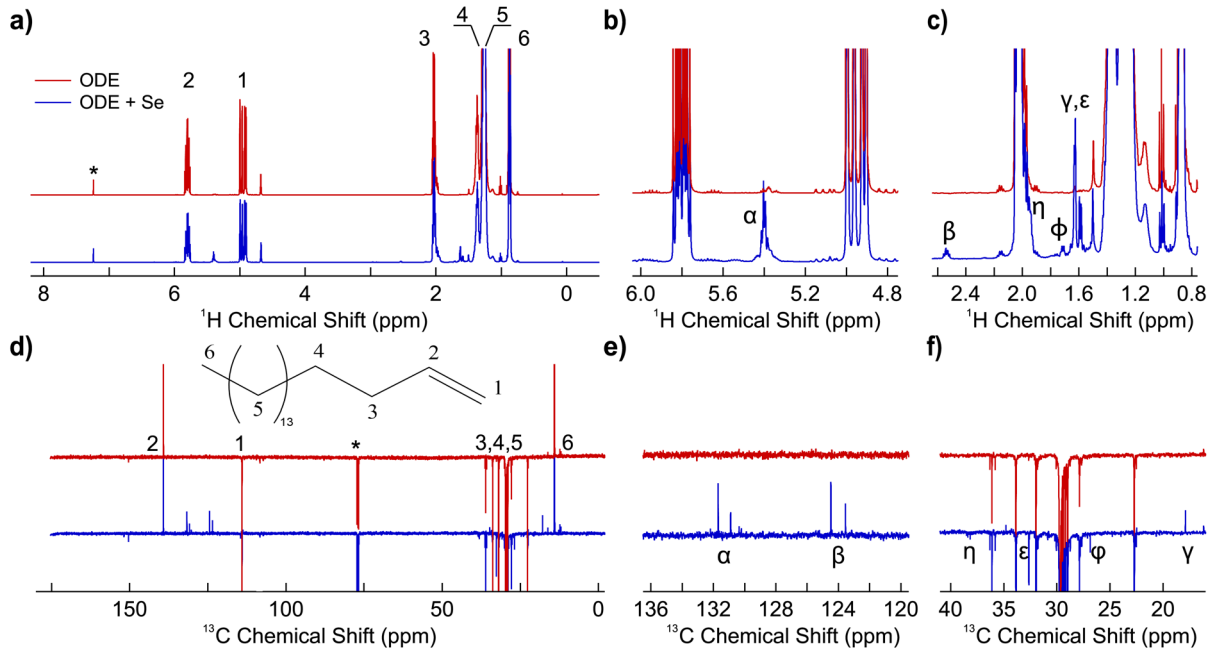

Fig. 2 (a) ^{1}H NMR ($CDCl_3$) spectra of ODE (red) and of the heated mixture ODE–Se (blue) and (b) and (c) magnifications on two regions of (a), showing the emergence of new signals. (d) APT ^{13}C NMR ($CDCl_3$) spectra of ODE (red) and of the heated mixture ODE–Se (blue) and (e) and (f) insets on two regions of (c) (* = residual solvent. α, β, γ, ε, η, ϕ new signals). The peak assignment follows the structure reported on top of panel (d).

lenium complex (*vide infra*). Finally, the multiplet centered around 2.5 ppm (β in Fig. 2c) can be assigned to a CH_2 in α position to a double bond of an organo-chalcogen species. Note that this peak also appears in the work of Bullen *et al.*, however, it was not further investigated.[20] In conclusion, the analysis of the ^{1}H spectra points toward the isomerization of 1-ODE and the formation of related organo-selenium complexes. It has been proposed that the chalcogen behaves as a hydrogen transfer agent.[18] This means that its interaction with C=C double bonds is expected to be similar to the one of dioxygen, with the isomerization of the double bond proceeding *via* a radical mechanism.[18,20,44]

A similar conclusion can be drawn from the analysis of the ^{13}C attached proton test (APT) NMR spectra of the same species, as shown in Fig. 2d–f. ^{13}C APT is routinely used in organic synthesis as it allows to encode the multiplicity *n* of the different $-CH_n$ units in a compound into a positive (for CH/CH_3) or negative (for CH_2/C_q) signal phase, adding relevant structural information compared to a regular 1D ^{13}C.[47] The presence of new positive signals in the region 123.6 ppm–131.7 ppm (α, β, Fig. 2e) is compatible with the formation of =CH moieties, as the two groups of signals (123.6–124.5 ppm and 130.9–131.7 ppm) can be related to the migration of the double bond along the aliphatic chain, as a consequence of the proposed radical mechanism.[18,20,44] In addition, the two negative signals at 32.6 and 26.9 ppm (ε, ϕ in Fig. 2f) can be attributed to CH_2 in α and β position to a double bond, respectively. Finally, the positive signal around 18.2 ppm (γ in Fig. 2f) can be assigned to a CH_3 in α position to a double bond. To sum up, chemical-shift based analysis of the 1D NMR experiments support that, in our synthesis conditions, selenium acts as a hydrogen transfer agent, promoting the isomerization of the alkene and the formation of activated organoselenium complexes. The chemical shifts of the emerging species are summarized in Table 1.

To confirm this analysis and reveal the underlying structure of the newly formed molecules, we have also registered 2D NMR experiments. The heteronuclear single quantum correlation (HSQC) spectra of the heated mixture of ODE and Se is shown in ESI, Fig. S3.† Protons with signals around 5.4 ppm (β in Fig. 2) are bound to the emerging =CH with ^{13}C signals in the region 123.6 ppm–131.7 ppm (α, β in Fig. 2e). This is in agreement with the double-bond isomerization (*e.g.*, 2-ODE, 3-ODE) and related organoselenium complexes. The coupling between the new Hγ doublet and the Cγ (Fig. 2) suggests the formation of a CH_3 in α position to a double bond (*e.g.*, 2-ODE) and associated organoselenium complex. This is also in agreement with the COSY spectrum (ESI, Fig. S4†), where the new Hα signal is adjacent to the Hγ and Hη (Fig. 2c) as it would be for 2-ODE.

To ensure that the new NMR signals were arising from the ODE-chalcogen interaction, we performed another control reaction. Working in the same conditions as in eqn (2), we heated ODE alone at 220 °C. The heating did not result in an evident colour change (ESI, Fig. S2†) and the proton and carbon NMR spectra did not show significant differences from the pristine ODE (ESI, Fig. S5†). This conveys that the newly formed signals are due to the interaction between the alkene and selenium.

We summarize our experimental results and propose the possible reactive ODE–Se precursor for our CdSe NPL synthesis in Fig. 3. It agrees well with the assignment of Bullen *et al.*,[20] who observed the same species in the CdSe quantum dot synthesis. We confirmed this structure with liquid and gas chromatography coupled to mass spectrometry (LC-MS and GC-MS, respectively). The LC-MS profile (ESI, Fig. S6†) shows a peak at m/z = 663, which can be assigned to the $[M + H]^+$ ion of a species containing 2 Se + 2 ODE fragments (Fig. S6†).[20] When we look at the GC-MS profile and its related fractions (ESI, Fig. S7 and S8†), a second species possesses a peak at m/z = 252 (ESI, Fig. S7†), which is attributable to 1-ODE and its isomers (*e.g.* 2-ODE, 3-ODE *etc.*). Additional components can be discerned with m/z = 250 (ESI, Fig. S8†), probably due to the formation of conjugated diolefins deriving from subsequent ODE dehydrogenation (*e.g.*, octadec-di-enes). From both NMR and MS, we can thus conclude that, for the CdSe NPL synthesis, the presence of allylic positions to a double bond is an important reactive framework for selenium. Data reveal that the main components formed are 2-ODE, 3-ODE, and ODE–Se_x complexes as depicted in Fig. 3.

Since ODE-chalcogen mixtures were already used for colloidal nanocrystal synthesis, we have also prepared and used a ODE–Se suspension.[20] We again monitored the gas evolution during the precursor preparation, and a lead acetate paper test did not yield any evidence of H_2Se formation during the heating. Next, we performed a synthesis in identical conditions as in eqn (2), but using ODE–Se as chalcogen precursor and hexadecane as solvent. The absorption spectra (Fig. 4a) clearly support the formation of CdSe NPLs, which was confirmed by TEM (Fig. 4b). Also during the synthesis, lead acetate tests did not evidence any evolution of H_2Se. This shows that we prepared a similar Se precursor as in typical NPL synthesis in

Table 1 Summary of the chemical shifts positions for the new NMR signals emerging from the heated ODE–Se mixture – the signals are shown in Fig. 2 and refer to the nomenclature in Fig. 3

Nucleus	α	β	η	ε	ϕ	γ
^{1}H (ppm)	5.40	2.54	1.96	1.59	1.71	1.63
^{13}C (ppm)	132.2	125.0	36.5	33.1	27.3	18.3

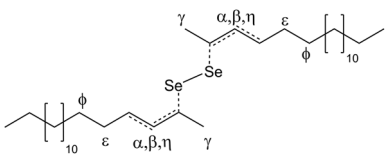

Fig. 3 Proposed structure for the reactive species forming during heating of ODE and selenium at 220 °C. The dashed lines refer to a variety of possible isomers (either for the selenium species or for the C=C double bond) hypothesized following the experimental results.

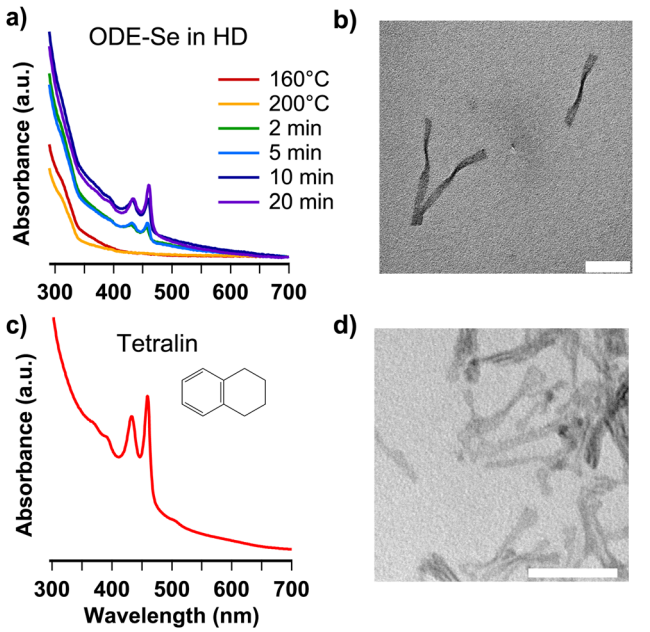

Fig. 4 (a) Temporal evolution of the absorption spectra of aliquots collected during a modified version of procedure in eqn (2), using *n*-hexadecane (HD) as solvent and the ODE–Se reagent as chalcogen source and (b) TEM image of the final particles obtained. (c) Absorption spectrum of NPLs obtained by a modified version of procedure (2), using tetralin (molecular structure in inset) as solvent. (d) TEM of the final particles obtained (scale bar equals 50 nm in both TEM images).

ODE (eqn (2) and Fig. 1a), but now using an *ex situ* method. In this case, HD can replace ODE as solvent.

The NMR results demonstrate that an alkene possessing allylic protons behaves as hydrogen transfer agent,[18,19] enabling the formation of reactive selenium. With this in mind, we used an aromatic solvent, 1,2,3,4-tetrahydronaphthalene (commonly known as tetralin), as solvent for an NPL synthesis. The solvent possesses a relatively high boiling point (b.p. = 207 °C), has a lower tendency to polymerize when compared to ODE and it has been used as an additive to reduce the average molecular weight of polymers.[48] These features are potentially beneficial for the subsequent nanocrystals purification. To test the reactivity of tetralin, we have conducted a synthesis following the procedure in eqn (2) using this solvent. The absorption spectrum and TEM image of NPLs grown for 30 minutes are shown in Fig. 4c and d. Also in this case, the absorption spectra of the aliquots can be attributed to 3.5 ML NPLs, and the TEM analysis confirms NPL formation. Once again, a radical reaction pathway can be expected, based upon literature results.[18,19,44,45] Given the lower self-polymerization tendency, tetralin is a promising solvent for NPLs that do not require temperatures above 207 °C for their synthesis. We can conclude that both linear alkene and aromatic solvents are suitable for the synthesis of CdSe NPLs, the only prerequisite being the presence of extractable protons in α to a C=C double bond.

While we have shown that the synthesis of CdSe NPLs is strongly impacted by the choice of the solvent, some NPL formation was still observed in a saturated alkane such as HD. In this respect, Riedinger *et al.* recently showed that CdSe NPLs can be obtained in a melt of cadmium carboxylate and selenium, hypothesizing that selenium acylates (or acylselenides, $(ROC)_2Se$, see Fig. 6a) are the reactive chalcogen species.[49,50] Additionally, they prepared $(ROC)_2Se$ with different organic backbones R and used them in an NPL synthesis[49] with ODE as a solvent, and in the synthesis of CdSe clusters with HD as a solvent.[39,51]

To explore this reaction pathway, we heated up a mixture of selenium and octanoic acid (OctAc, b.p. = 237 °C) at 220 °C and investigated the products formed. As an excess of octanoic acid, and even propionic acid,[34] are used in our synthesis, one can assume that either (or both) may interact with selenium. During heating, we observed a color transition from grey to deep orange (ESI, Fig. S9†). This is already similar to what was observed in the heated ODE–Se mixture. The suspension turns pale yellow after cooling to room temperature, together with the separation of a red solid, probably red selenium.[18,19,45,52] ^{1}H and ^{13}CNMR spectra were collected from the reaction supernatant, and are shown in Fig. 5 together with the spectrum of pristine octanoic acid. In the ^{1}H spectrum, a new resonance appears around 2.42 ppm (α in Fig. 5b), with an intensity comparable to the ^{13}C satellites of the main octanoic acid α CH_2 peak, located at 2.32 ppm. The ^{13}C NMR spectrum is shown in Fig. 5d–f Also here, after heating, two new signals, around 35.3 and 24.2 ppm (α and β, respectively) appear. These can be assigned to new carbons in α and β position to a new C=O moiety. A new signal emerging around 169 ppm (γ in Fig. 5) can be assigned to a quaternary carbon. The new signals are summarized in Table 2. We also ran a control reaction, heating octanoic acid alone at 220 °C. The final product was again analyzed *via* NMR spectroscopy. New signals appear in the ^{1}H and ^{13}C spectra of the heated mixture, at similar chemical shift, yet with reduced intensity (ESI, Fig. S10†).

Interestingly, comparing our results with the chemical shifts reported by Riedinger *et al.*[49] for acylselenide, we observe key differences. In our case, the chemical shifts of the OctAc–Se mixture and the heated octanoic acid sample can be assigned to octanoic anhydride (spectral database for organic compounds (SDBS),[53] no.: 7738). While it is clear from Riedinger *et al.*[49] that acylselenides are a viable Se precursor, we do not find evidence for its formation when heating octanoic acid with selenium, which instead may be activated *via* formation of a complex with the anhydride. In Fig. 6b we show the possible structure of the selenium complex, taking the formation of anhydrides into account. To demonstrate that it can also lead to the formation of NPLs, we ran a control reaction, using the heated OctAc–Se as precursor. We observed that 3.5 NPLs are indeed formed, together with a sizeable fraction of 0D quantum dots (ESI, Fig. S11†), hence, it is clear that, at high temperatures, selenium forms a reactive complex with organic acids such as octanoic acid, further enriching the Se precursors present during NPL synthesis.

Finally, adaptation of the synthesis conditions (see Methods section) can also yield NPLs with different thickness.

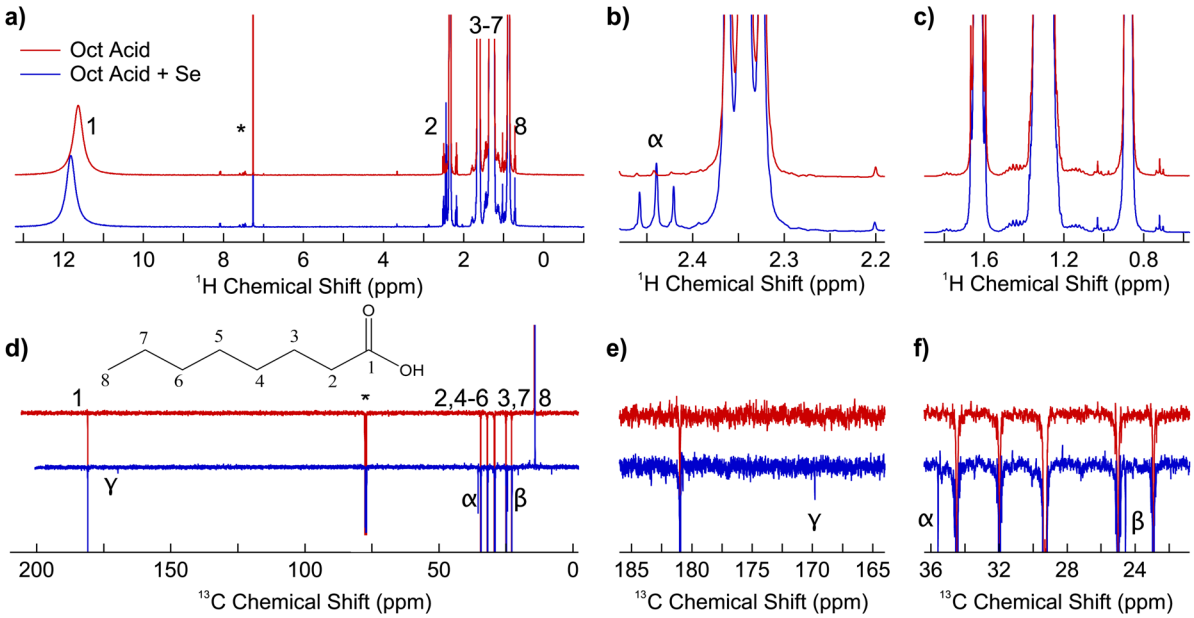

Fig. 5 (a) ^{1}H NMR ($CDCl_3$) spectra of pristine octanoic acid (red) and of the heated octanoic acid–Se mixture (blue) and (b) and (c) magnifications on two regions of (a), showing the emergence of new signals. (d) APT ^{13}C NMR ($CDCl_3$) spectra of pristine octanoic acid (red) and of the heated octanoic acid–Se mixture (blue) and (e) and (f) magnifications on two regions of (c). (* = residual solvent. α, β, γ: new signals). The peak assignment follows the structure reported on top of panel (d).

Table 2 Summary of the chemical shift positions for the new NMR signals emerging from the heated OctAc–Se mixture – the signals are shown in Fig. 5 and refer to the nomenclature in Fig. 6b

Nucleus	α	β	γ
^{1}H (ppm)	2.42	—	—
^{13}C (ppm)	35.3	24.2	169.0

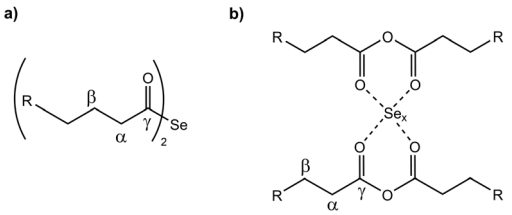

Fig. 6 Proposed selenium reactive species in NPLs syntheses. (a) Acylselenides (as proposed in ref. 49). (b) Selenium complexation by anhydrides formed *in situ* (x = 1, 2, ..., refers to the possibility of formation of multinuclear Se–Se structures).

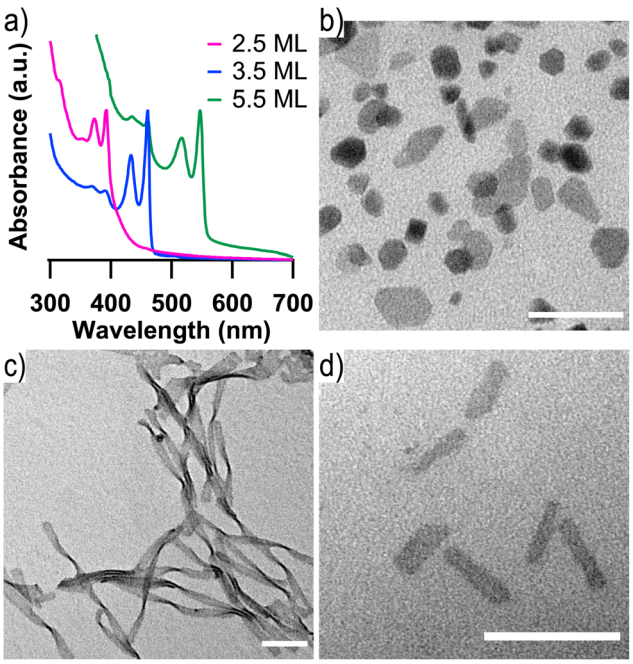

Fig. 7 Synthesis of different NPL thicknesses (a) absorbance spectra of 2.5 ML (pink), 3.5 ML (blue) and 5.5 ML (green) NPLs. (b–d) TEM images of 2.5 ML NPLs (b), 3.5 ML NPLs (c) and 5.5 ML NPLs (d). The scale bars equal 50 nm.

For instance, we already observed that a synthesis in HD yields mostly 2.5 ML NPLs (Fig. 1b). When performing the reaction in HD, using elemental Se, and lowering the growth temperature to 190 °C, we obtained 2.5 ML NPLs (Fig. 7a and b). Interestingly, in contrast with our previous results, where we obtained extended nanosheets by growth at 160 °C,[34] here we obtained substantially smaller NPLs, with average width and length of 9 nm by 27 nm (ESI, Fig. S12† for the associated histograms). Additionally, Fig. 1d shows that a reaction performed in HD with 0.5 mmol of ODE, using elemental Se, already yields a sizeable fraction of 3.5 ML NPLs after 20 minutes. Considering that this fraction increases by Ostwald ripening and digesting of the 2.5 ML NPLs,[43] by

simply extending the growth time, here to 185 minutes, we could obtain nanoribbon-like 11 nm by *ca.* 150 nm 3.5 ML NPLs (Fig. 7a, c and ESI, Fig. S12†). Finally, with a slight modification of the precursor concentrations with respect to the synthesis of Singh *et al.*,[54] we could obtain 5 nm by 24 nm 5.5 ML NPLs, grown in a solvent mixture of HD with 0.6 mmol of ODE, using elemental Se (Fig. 7a, d and ESI, Fig. S12†). Note that further optimization may still be possible, as the crude product was polydisperse (ESI, Fig. S13†), however, careful purification largely removed the undesired fractions.

Conclusion

In this work, we have explored the reactivity of the different components that lead to the synthesis of CdSe NPLs. Starting from the role of the dispersive medium and from literature reports, we have shown that the role of the typical solvent, ODE, is often overlooked. By combining NMR and MS analyses we confirmed that the carbon–carbon double bond moiety reacts with selenium, allowing for the reduction (and thus activation) of the chalcogen. As we have found no evidence of reaction between selenium and textitn-hexadecane (HD), we have used this solvent to exploit the alkene reactivity in different syntheses, either spiking HD with known amounts of ODE, or using a ODE–Se reagent prepared beforehand. We show that is it possible to reduce the amount of ODE injected in the colloidal synthesis. No clear evidence of H_2Se formation was observed, and *via* NMR and MS studies, we infer that the improved reactivity is due to organo-selenium complexes arising from chalcogen-alkene interaction and the isomerization of the carbon–carbon double bond provided by available allylic protons. This concept was exploited to obtain NPLs using tetralin as solvent, with results similar to ODE. We believe that the dispersive medium should be considered as one of the reagents in the synthesis, unless proven otherwise. Given that NPLs could still be obtained in HD, we have then shifted our attention to the reaction between carboxylic acids and selenium. *Via* NMR spectroscopy we show that the two species can interact, likely leading to selenium-anhydride complexes. Our results were adapted to grow a variety of CdSe thicknesses, and can lead to rationalization of the chemistry underlying the colloidal synthesis of 2D nanocrystals.

Conflicts of interest

There are no conflicts to declare.

Acknowledgements

This project has received funding from the European Research Council (ERC) under the European Union's Horizon 2020 research and innovation program (grant agreement no. 714876 PHOCONA) and the Research Foundation – Flanders (grant no. G037221N). TEM measurements were performed at the UGent TEM Core Facility. We thank the NMR expertise centre (Ghent University) for providing support and access to its NMR infrastructure. The 500 MHz equipment used in this work has been funded by the Hercules Foundation and UGent (grant code AUGE09/006).

References

1 C. B. Murray, D. J. Norris and M. G. Bawendi, *J. Am. Chem. Soc.*, 1993, **115**, 8706–8715.
2 J. M. Pietryga, Y.-S. Park, J. Lim, A. F. Fidler, W. K. Bae, S. Brovelli and V. I. Klimov, *Chem. Rev.*, 2016, **116**, 10513–10622.
3 F. P. García de Arquer, D. V. Talapin, V. I. Klimov, Y. Arakawa, E. H. Bayer and M. Sargent, *Science*, 2021, **373**, eaaz8541.
4 M. D. Tessier, K. De Nolf, D. Dupont, D. Sinnaeve, J. De Roo and Z. Hens, *J. Am. Chem. Soc.*, 2016, **138**, 5923–5929.
5 H. Liu, J. S. Owen and A. P. Alivisatos, *J. Am. Chem. Soc.*, 2007, **129**, 305–312.
6 M. P. Hendricks, M. P. Campos, G. T. Cleveland, I. J.-L. Plante and J. S. Owen, *Science*, 2015, **348**, 1226–1230.
7 W. Yin, H. Li, A. S. R. Chesman, B. Tadgell, A. D. Scully, M. Wang, W. Huang, C. R. McNeill, W. W. H. Wong, N. V. Medhekar, P. Mulvaney and J. J. Jasieniak, *ACS Nano*, 2021, **15**, 1454–1464.
8 Z. Hens and R. K. Čapek, *Coord. Chem. Rev.*, 2014, **263–264**, 217–228.
9 J. S. Owen, E. M. Chan, H. Liu and A. P. Alivisatos, *J. Am. Chem. Soc.*, 2010, **132**, 18206–18213.
10 W. W. Yu and X. G. Peng, *Angew. Chem., Int. Ed.*, 2002, **41**, 2368–2371.
11 C. R. Bullen and P. Mulvaney, *Nano Lett.*, 2004, **4**, 2303–2307.
12 J. Park, K. H. Lee, J. F. Galloway and P. C. Searson, *J. Phys. Chem. C*, 2008, **112**, 17849–17854.
13 J. E. Mark, B. Erman and M. Roland, *The science and technology of rubber*, Academic Press, 3rd edn, 2013.
14 J. Jasieniak, C. Bullen, J. van Embden and P. Mulvaney, *J. Phys. Chem. B*, 2005, **109**, 20665–20668.
15 G. G. Yordanov, H. Yoshimura and C. D. Dushkin, *Colloid Polym. Sci.*, 2008, **286**, 813–817.
16 C. Pu, J. Zhou, R. Lai, Y. Niu, W. Nan and X. Peng, *Nano Res.*, 2013, **6**, 652–670.
17 Z. Deng, L. Cao, F. Tang and B. Zou, *J. Phys. Chem. B*, 2005, **109**, 16671–16675.
18 W. T. House and M. Orchin, *J. Am. Chem. Soc.*, 1960, **82**, 639–642.
19 H. A. Silverwood and M. Orchin, *J. Org. Chem.*, 1962, **27**, 3401–3404.
20 C. Bullen, J. van Embden, J. Jasieniak, J. E. Cosgriff, R. J. Mulder, E. Rizzardo, M. Gu and C. L. Raston, *Chem. Mater.*, 2010, **22**, 4135–4143.
21 M. Nasilowski, B. Mahler, E. Lhuillier, S. Ithurria and B. Dubertret, *Chem. Rev.*, 2016, **116**, 10934–10982.

22 M. D. Tessier, C. Javaux, I. Maksimovic, V. Loriette and B. Dubertret, *ACS Nano*, 2012, **6**, 6751–6758.
23 J. Q. Grim, S. Christodoulou, F. Di Stasio, R. Krahne, R. Cingolani, L. Manna and I. Moreels, *Nat. Nanotechnol.*, 2014, **9**, 891–895.
24 B. T. Diroll, D. V. Talapin and R. D. Schaller, *ACS Photonics*, 2017, **4**, 576–583.
25 C. She, I. Fedin, D. S. Dolzhnikov, A. Demortiere, R. D. Schaller, M. Pelton and D. V. Talapin, *Nano Lett.*, 2014, **14**, 2772–2777.
26 Y. Kelestemur, Y. Shynkarenko, M. Anni, S. Yakunin, M. L. De Giorgi and M. V. Kovalenko, *ACS Nano*, 2019, **13**, 13899–13909.
27 U. Giovanella, M. Pasini, M. Lorenzon, F. Galeotti, C. Lucchi, F. Meinardi, S. Luzzati, B. Dubertret and S. Brovelli, *Nano Lett.*, 2018, **18**, 3441–3448.
28 M. İzmir, A. Sharma, S. Shendre, E. G. Durmusoglu, V. K. Sharma, F. Shabani, H. D. Baruj, S. Delikanli, M. Sharma and H. V. Demir, *ACS Appl. Nano Mater.*, 2022, **5**, 1367–1376.
29 G. H. Bertrand, A. Polovitsyn, S. Christodoulou, A. H. Khan and I. Moreels, *Chem. Commun.*, 2016, **52**, 11975–11978.
30 Z. Li and X. Peng, *J. Am. Chem. Soc.*, 2011, **133**, 6578–6586.
31 S. Christodoulou, J. I. Climente, J. Planelles, R. Brescia, M. Prato, B. Martin-Garcia, A. H. Khan and I. Moreels, *Nano Lett.*, 2018, **18**, 6248–6254.
32 N. Moghaddam, C. Dabard, M. Dufour, H. Po, X. Xu, T. Pons, E. Lhuillier and S. Ithurria, *J. Am. Chem. Soc.*, 2021, **143**, 1863–1872.
33 W. Cho, S. Kim, I. Coropceanu, V. Srivastava, B. T. Diroll, A. Hazarika, I. Fedin, G. Galli, R. D. Schaller and D. V. Talapin, *Chem. Mater.*, 2018, **30**, 6957–6960.
34 A. Di Giacomo, C. Rodà, A. H. Khan and I. Moreels, *Chem. Mater.*, 2020, **32**, 9260–9267.
35 D. E. Yoon, J. Lee, H. Yeo, J. Ryou, Y. K. Lee, Y. H. Kim and D. C. Lee, *Chem. Mater.*, 2021, **33**, 4813–4820.
36 S. Ithurria, M. D. Tessier, B. Mahler, R. P. Lobo, B. Dubertret and A. L. Efros, *Nat. Mater.*, 2011, **10**, 936–941.
37 E. Dhaene, J. Billet, E. Bennett, I. Van Driessche and J. De Roo, *Nano Lett.*, 2019, **19**, 7411–7417.
38 M. Calcabrini, D. Van den Eynden, S. Sánchez Ribot, R. Pokratath, J. Llorca, J. De Roo and M. Ibánez, *JACS Au*, 2021, **1**, 1898–1903.
39 A. B. Pun, A. S. Mule, J. T. Held and D. J. Norris, *Nano Lett.*, 2021, **21**, 7651–7658.
40 S. Ithurria, G. Bousquet and B. Dubertret, *J. Am. Chem. Soc.*, 2011, **133**, 3070–3077.
41 D. A. Kurtina, A. V. Garshev, I. S. Vasil'eva, V. V. Shubin, A. M. Gaskov and R. B. Vasiliev, *Chem. Mater.*, 2019, 9652–9663.
42 S. Delikanli, G. Yu, A. Yeltik, S. Bose, T. Erdem, J. Yu, O. Erdem, M. Sharma, V. K. Sharma, U. Quliyeva, S. Shendre, C. Dang, D. H. Zhang, T. C. Sum, W. Fan and H. V. Demir, *Adv. Funct. Mater.*, 2019, 1901028–1901037.
43 P. N. Knüsel, A. Riedinger, A. A. Rossinelli, F. D. Ott, A. S. Mule and D. J. Norris, *Chem. Mater.*, 2020, **32**, 3312–3319.
44 B. Hou, D. Benito-Alifonso, R. Webster, D. Cherns, M. C. Galan and D. J. Fermín, *J. Mater. Chem. A*, 2014, **2**, 6879–6886.
45 J. D. Fitzpatrick and M. Orchin, *J. Am. Chem. Soc.*, 1957, **79**, 4765–4771.
46 G. G. Yordanov, C. D. Dushkin, G. D. Gicheva, B. H. Bochev and E. Adachi, *Colloid Polym. Sci.*, 2005, **284**, 229–232.
47 H. Günther, *NMR spectroscopy: basic principles, concepts and applications in chemistry*, John Wiley & Sons, 2013.
48 G. Madras, J. M. Smith and B. J. McCoy, *Ind. Eng. Chem. Res.*, 2002, **34**, 4222–4228.
49 A. Riedinger, A. S. Mule, P. N. Knusel, F. D. Ott, A. A. Rossinelli and D. J. Norris, *Chem. Commun.*, 2018, **54**, 11789–11792.
50 M. Koketsu, F. Nada, S. Hiramatsu and H. Ishihara, *J. Chem. Soc., Perkin Trans. 1*, 2002, 737–740.
51 A. B. Pun, S. Mazzotti, A. S. Mule and D. J. Norris, *Acc. Chem. Res.*, 2021, **54**, 1545–1554.
52 O. Foss and V. Janickis, *J. Chem. Soc., Dalton Trans.*, 1980, 624–627.
53 National Institute of Advanced Industrial Science and Technology, January 2024, **https://sdbs.db.aist.go.jp**.
54 S. Singh, R. Tomar, S. Ten Brinck, J. De Roo, P. Geiregat, J. C. Martins, I. Infante and Z. Hens, *J. Am. Chem. Soc.*, 2018, **140**, 13292–13300.